Transformer 2β Regulates the Alternative Splicing of Cell Cycle Regulator Genes to Promote Ovarian Cancer Cell Progression

Peiying Fu
Tongji Hospital of Tongji Medical College of Huazhong University of Science and Technology
Ting Zhou
Tongji Hospital of Tongji Medical College of Huazhong University of Science and Technology
Dong Chen
ABLife BioBigData Institute
ShiXuan Wang
Tongji Hospital of Tongji Medical College of Huazhong University of Science and Technology
Ronghua Liu (liuzhu@126.com)
Tongji Hospital of Tongji Medical College of Huazhong University of Science and Technology
https://orcid.org/0000-0002-4197-3971

Research

Keywords: TRA2B, CYR61, HMGA2, RNA binding proteins, splicing, ovarian cancer

Posted Date: September 14th, 2021

DOI: https://doi.org/10.21203/rs.3.rs-853170/v1

Abstract

Background: Late-stage ovarian cancer (OV) has a poor prognosis and a high metastasis rate, but the underlying molecular mechanism is ambiguous. RNA binding proteins (RBPs) play important roles in posttranscriptional regulation in the contexts of neoplasia and tumor metastasis.

Results: In this study, we explored the molecular functions of a canonical RBP, TRA2B, in cancer cells. TRA2B knockdown in HeLa cells and whole-transcriptome sequencing (RNA-seq) experiments revealed that the TRA2B-regulated alternative splicing (AS) profile was tightly associated with the mitotic cell cycle, apoptosis, and several cancer pathways. Moreover, hundreds of genes were regulated by TRA2B at the expression level, and their functions were enriched in cell proliferation, cell adhesion and angiogenesis, which are related to cancer progression. We also observed that AS regulation and expression regulation occurred independently by integrating the alternatively spliced and differentially expressed genes. We then explored and validated the carcinogenic functions of TRA2B by knocking down its expression in OV cells. In vivo, a high expression level of TRA2B was associated with a poor prognosis in OV patients. **Conclusions:** We demonstrated the important roles of TRA2B in ovarian neoplasia and OV progression and identified the underlying molecular mechanisms, facilitating the targeted treatment of OV in the future.

Background

Ovarian cancer (OV) is the most common cause of gynecological cancer-associated death in postmenopausal women. Surgery and platinum-based cytotoxic chemotherapy treatment for advanced OV are often futile and can cause deformation of the body [1]. Therefore, early detection of OV is the top priority. Genetic mutations of key genes, including BRAF, KRAS, PTEN, P53 and BRCA1/2, are regarded as potential molecular causes of OV [2]. As master regulators of posttranscriptional regulation, RNA binding proteins (RBPs) play a crucial role in RNA metabolism and regulatory RNA splicing, localization, monitoring, degradation and translation [3, 4]. Since RBPs participate in the regulation of various splicing changes in cancers, they can contribute to several cancer hallmarks through effects on the expression patterns of important protein isoforms that regulate cell behavior [5]. However, the functions of RBPs in OV are largely unknown.

Transformer 2 β homolog (TRA2B), also known as SFRS10 or SRFS10, is a member of the serine/arginine (S/R)-rich splicing factor (SRSF) family and was initially recognized as an important regulator of sex determination in insects [6–8]. TRA2B and TRA2A are homologous genes in the long arm of human chromosome 7. TRA2A is copied from the TRA2B gene early in the vertebrate lineage, and therefore, they are conserved across the animal kingdom [9]. It has been reported that serine phosphorylation is important for the activity and subnuclear localization of TRA2B [10, 11]. As canonical RBPs, transformer proteins control the fate of target RNAs by regulating primary RNA alternative splicing (AS) and RNA degradation[12]. In addition to its sex-determination functions, TRA2B is involved in other biological processes, including metabolism [13, 14] and development [15, 16]. A recent study demonstrated that

Tra2α and Tra2β jointly control constitutive splicing and AS patterns via paralog compensation [17]. Above all, these results suggest that TRA2B is a multifunctional protein and that its functions in development and disease should be further explored.

Several studies have revealed that TRA2B can inhibit cancer cell apoptosis or promote invasion in several cancers [18, 19]. Both TRA2B RNA and Tra2β protein levels are upregulated in many cancers [20]. The identified pro-oncogenic splicing targets of Tra2β include CD44 [21], HipK3 [22], and Nasp-T [23]. Increased protein and mRNA levels of SR proteins, including Tra2β and YB−1, were observed in malignant OV tissue [24]. A recent study considered TRA2B as a proto-oncogene that may contribute to the difference in the expression of CYR61, which is related to the proliferation and apoptosis of cancer cells [25]. Thus, exploring how TRA2B functions in OV cells may greatly contribute to our knowledge of OV.

In this study, we used next-generation RNA sequencing (RNA-seq) technology to systematically investigate global TRA2B-regulated alternative splicing events (RASEs) and global gene expression changes by silencing the expression of TRA2B in cancer cells. We found that TRA2B could extensively regulate gene expression and AS in HeLa cells, which was highly related to its carcinogenic functions. Silencing experiments of TRA2B in ovarian cells validated its functions in cell proliferation, cell invasion and cell apoptosis in OV cells. In summary, we extensively confirmed that TRA2B exerts carcinogenic functions in OV cells by regulating the expression and AS of associated genes.

Results

TRA2B promotes OV progression

As a splicing factor, TRA2B plays important roles in multiple biological processes, while its functions and molecular mechanisms in OV are not clear. We constructed a TRA2B regulatory network by performing coexpression analysis (Pearson correlation coefficient ≥ 0.6 and p-value ≤ 0.05). We found that TRA2B was coexpressed with genes involved in cell proliferation and apoptosis, transcription regulation and gene expression (top enriched terms, Fig. 1A). By utilizing the transcriptome data of OV from The Cancer Genome Atlas (TCGA) database, we found that TRA2B first increased and then decreased as OV stage increased (Fig. 1B), indicating its regulatory role in OV development. Overall survival (OS) and progression-free survival (PFS) analysis of TRA2B in OV by KM plotter demonstrated that OV patients with higher TRA2B expression levels globally had shorter survival times than patients with lower TRA2B expression levels ($p = 0.00072$ and $p = 0.038$) (Fig. 1C-D). To further explore the molecular functions of TRA2B in OV, we selected the top 20 and bottom 20 OV samples by ranking TRA2B expression levels to analyze TRA2B-regulated genes and AS events. DEG analysis obtained 3231 and 2518 upregulated and downregulated genes by TRA2B, respectively. Functional enrichment analysis revealed that mitotic cell cycle and DNA replication terms were significantly enriched in upregulated genes (Fig. 1E), while cell adhesion and immune/inflammatory response terms were significantly enriched in downregulated genes (Fig. 1F), indicating the potential molecular functions of TRA2B in OV. We then analyzed TRA2B RASEs and the functions of regulated AS genes (RASGs). We found that mitotic cell cycle-related terms were

also enriched in RASGs (Fig. 1G). There were 671 genes whose expression and AS patterns were affected by TRA2B. Functional terms including mitotic cell cycle, DNA replication, cell adhesion, and extracellular matrix disassembly were enriched for both the DEGs and the RASGs (Fig. 1H). In summary, the results from TCGA OV transcriptome data indicated that TRA2B could promote OV development by regulating the cell cycle and cell adhesion at the transcriptional or posttranscriptional level.

TRA2B-regulated genes are involved in multiple cancer-related functions

To further identify the molecular mechanism of TRA2B-mediated transcriptional regulation, we constructed a cell model by knocking down TRA2B using shRNA in HeLa cells. We examined the expression of TRA2B in HeLa cells transduced with two different empty vectors or shRNAs of TRA2B by RT-qPCR. We chose HeLa cells for these experiments for the following reasons: studies have shown that HeLa cells are model cells for studying RBPs [26, 27], and HeLa cells are good for gene regulation studies involving cancer molecular mechanisms [28, 29]. RT-qPCR showed that 48 h after transfection, TRA2B gene expression had a 60% cutoff in shRNA-transfected cells (Fig. 2A). We then constructed cDNA libraries on shTRA2B and control cells for RNA-sEq. Two biological replicates were prepared for shTRA2B and control samples. After aligning the quality filtered reads to the human GRCH38 genome sequence, fragments per kilobase per million (FPKM) values were calculated and used as the expression level for each identified gene. The effective consumption of TRA2B was also confirmed by parallel RNA-seq analysis (Fig. 2B). Gene expression levels were used to calculate a correlation matrix based on Pearson's correlation coefficient. The hierarchical clustering heat map of sample correlations showed that shTRA2B samples were clearly separated from control samples and that the biological replicates were highly correlated (Fig. 2C), indicating that TRA2B knockdown treatment was successful and altered the global expression profile.

To explore the gene expression impact of shTRA2B in HeLa cells, we performed DEG analysis between shTRA2B and control samples. We ran the two most commonly used R packages, edgeR and DESeq, to perform this analysis. FDR < 0.05 and FC > 2 or FC < 0.5) were used as the DEG thresholds. We obtained 1507 upregulated and 986 downregulated genes by edgeR and 214 upregulated and 177 downregulated genes by DESEq. Overlap analysis of these DEGs predicted by these two methods showed that almost all of the DEGs detected by DESeq were included in DEGs detected by edgeR (Fig. 2D), except 4 downregulated genes, indicating the high consistency between these two methods. However, the many more DEGs detected by edgeR failed to meet the DEG criteria of DESEq. By analyzing the cumulative expression curve of DEGs, we found that DEGs detected by edgeR showed a significantly lower expression level than DEGs detected by DESeq (Fig. 2E). To keep increase the credibility of our results, we used the DEG results detected by DESeq in the following analysis.

We then analyzed the enriched functions of DEGs by performing GO and KEGG enrichment analysis. Among the biological process (BP) terms of GO analysis of the genes upregulated by shTRA2B, glucose homeostasis and small GTPase-mediated signal transduction were ranked at the top. The oxidation –

reduction process and angiogenesis were also included in the enriched BP terms (Fig. 2F). These metabolism and developmental terms were highly related to cancer development [30]. For the downregulated genes, angiogenesis, positive regulation of the apoptotic process, and positive regulation of cell proliferation were the most enriched (Fig. 2G), are these processes also closely related to cancer hallmarks [31]. These results together suggest that TRA2B knockdown in HeLa cells could greatly regulate the expression of cancer-related genes.

TRA2B-mediated regulation of angiogenesis- and apoptosis-related gene expression and the relationship between these genes and the prognosis of patients with OV

Next, we selected the downregulated genes with the most significant FDR values from the top ten enriched GO BP terms and presented them in the volcano plot; these included CYR61, SH2D2A, HMGA2, EPHB2, FN1, ETS1, CTGF, ANGPTL4, FOSL1, BCL2L1, ANPEP, and PVRL1 (Fig. 3A). Individual analysis of the expression levels of several main genes showed that they were highly and consistently downregulated after TRA2B knockdown (Fig. 3B). Specifically, the expression of CYR61 has been proven to be regulated by TRA2B via direct binding to the pre-mRNA of CYR61, which was consistent with our results. Three small siRNA fragments (siRNA 405, siRNA 581 and siRNA 798) were designed to screen and validate the most effective TRA2B siRNA in OV cells. The results showed that siRNA 798 had the most obvious inhibitory effect on TRA2B in OV cells (Fig. 3C). To further validate the influence of TRA2B knockdown on the expression of these genes, we performed Western blotting (WB) experiments to check their protein levels in OV cells. After TRA2B knockdown, the expression of CYR61, FN1, HMGA2, CTGF, ASAP3, ERBB3, IL-6, IL-1, JUN, MMP13, ODC1, and VEGFC in OV cells was increased. However, the expression of MAP2K6 and NPNT increased (Fig. 3D). We used KM plotter to analyze the survival status of OV patients with different expression levels of some major regulated genes (CYR61, FN1, HMGA2 and MAP2K6). OV patients with higher global CYR61, FN1 and HMGA2 expression levels had shorter survival times than patients with lower expression levels (Supplementary Fig. 1A-F). However, the trend for MAP2K6 was opposite to that of the above genes (Supplementary Fig. 1G-H).

Identification of TRA2B-dependent AS events

A key purpose of our study was to gain knowledge of the AS regulatory role of TRA2B. Therefore, transcriptome sequencing data were further analyzed to investigate the RASEs by TRA2B knockdown treatment. We used the ABLas program [32] to detect RASEs by TRA2B in HeLa cells. With AS ratio > 0.15 and p-value < 0.05 as thresholds, we detected 201 upregulated and 253 downregulated RASEs. TRA2B-regulated AS events included cassette exon (69)/exon skipping (86 ES), alternative 5' splice site (127 A5SS), and alternative 3' splice site (137 A5SS). These data suggested that TRA2B globally regulates AS events in HeLa cells. The other event types included 5pMXEs (n = 36), 3pMXEs (n = 17), MXEs (n = 29), A5SS&ES (n = 12) and A3SS&ES (n = 10) (Fig. 4A). These data indicated that TRA2B plays a role in the regulation of global AS events in HeLa cells.

It was further revealed that the genes regulated by TRA2B-mediated AS were highly enriched for chromosome segregation, mitosis, mitotic cell cycle, induction of apoptosis via death domain receptors, positive regulation of transcription, DNA – dependent, and gene expression (GO BP terms, Fig. 4B). Enriched KEGG pathways ($p < 0.05$) included those involved in pyrimidine metabolism, colorectal cancer, the cell cycle, and selenocompound metabolism (Fig. 4C). In contrast to the functional enrichment results of DEGs, we found that TRA2B-regulated AS genes were mainly enriched in cell cycle-related terms, showing high consistency with the TCGA data. Genes involved in the mitotic cell cycle included DSN1, MCM8, NSL1, CENPM, CDC16, CENPK, SKP1, SEC13, ANAPC11, UBA52, NEK9, NUP153, CLIP1, POLD4, CDK5RAP2, ESPL1, and RANBP2. Transcriptional regulation-related terms also emerged in GO BP terms for genes that were regulated by TRA2B at the AS level (Fig. 4B), including SMAD4, SMAD2, HNRNPC, HNRNPF, etc.

To illustrate the reliability of the RASE results, we selected four RASEs and corresponding genes to show their read density and statistical significance; these included SMAD4 (cassette exon, Fig. 5A), DSN1 (ES, Fig. 5B), MCM8 (A5SS, Fig. 5C), and UBE2I (A5SS, Fig. 5D). These four genes were related to the mitotic cell cycle or regulation of transcription terms, which were affected by TRA2B knockdown. In summary, these results suggest that TRA2B extensively regulates AS events in cancer cells.

TRA2B independently regulates gene expression and AS

To rule out the possibility that the increase in AS events is simply due to upregulation of transcription, we identified the overlapping genes whose expression level and AS were both regulated by TRA2B knockdown; six genes (Supplementary Fig. 2, p-value = 1, hypergeometric test), including VIPR2, EPHB2, TRA2B, TSC22D3, NPNT, and LINC00963, were identified. Interestingly, TRA2B knockdown promoted the exon 2 inclusion of its own transcript (Fig. 6A). The small overlap between DEGs and RASGs with TRA2B knockdown suggested that TRA2B could regulate gene expression and AS via independent functional mechanisms.

To further validate our hypothesis, we illustrated the read density profile of two CCN family proteins (CYR61 and CTGF). CYR61 and CTGF are known as important players in tumor progression, promoting neovascularization and metastasis [33–34]. From our results, we found that there were no RASEs in the intron 3 region of TRA2B from either control or shTRA2B samples (Fig. 6B, blue arrow). Similarly, for CTGF transcripts, no RASEs were detected in the read density plot (Fig. 6C).

TRA2B promotes cell proliferation and invasion and inhibits cell apoptosis in ovarian cell lines

To identify whether TRA2B affected cell proliferation, we observed the changes in the morphology of different OV cell lines after treatment with TRA2B shRNA, TRA2B siRNA 798, vector/control or PBS. Most HO8910 and A2780 cells exposed to TRA2B shRNA or TRA2B siRNA 798 became rounded and detached from the tissue culture plate. Minor morphological changes were detected in vector/control-treated cells compared with control cells (Fig. 7A, B, left panels). Then, we adopted the CCK-8 assay to verify OV cell

viability after treatment with TRA2B shRNA or TRA2B siRNA 798 for 0 h, 12 h, 24 h, 48 h or 72 h. The results showed that both TRA2B shRNA and TRA2B siRNA 798 had obvious cytotoxic effects on HO8910 and A2780 cells, respectively (Fig. 7A, B, right panels), which was correlated with the morphological changes induced by knockdown. Both TRA2B shRNA in HO8910 cells and TRA2B siRNA 798 in A2780 cells inhibited tumor cell proliferation in a time-dependent manner. In addition, to characterize whether TRA2B shRNA or TRA2B siRNA 798 induced apoptosis, the apoptotic rates of HO8910 and A2780 cells were analyzed using an annexin V/PI apoptosis assay. Our results showed that remarkable increases in apoptosis rates were detected in HO8910/TRA2B shRNA- and A2780/TRA2B siRNA 798 cells compared with vector/control-treated cells (Fig. 7C, D).

We next investigated whether TRA2B shRNA or TRA2B siRNA 798 could inhibit the migration of OV cells. The ability of cells to migrate was determined by Transwell tests and wound healing assays. As the Transwell assay results showed, TRA2B shRNA or TRA2B siRNA 798 inhibited the migratory abilities of OV cells (Fig. 8A, B). The wound healing assay showed that the downregulation of TRA2B shRNA or TRA2B siRNA 798 significantly inhibited the migration of OV cells (Supplementary Figure Fig. 3A, B).

Discussion

In this study, we used a transcriptome high-throughput sequencing method to explore the global expression and AS influences of TRA2B in human cancer cells and validated the cancer promotion functions of TRA2B in OV cells. Relatively high concentrations of hyperphosphorylated TRA2B protein isoforms were induced in OV, suggesting its potential functions in AS regulation of OV [35]. We also highlighted the expression-level regulatory functions of TRA2B in addition to its AS regulatory functions, and these two regulatory functions may be independent. By silencing TRA2B expression in OV cells, cell migration and proliferation were inhibited, while apoptosis was induced, validating the carcinogenic functions of TRA2B. Taken together, these results greatly expanded the knowledge regarding the functions and molecular mechanisms of TRA2B in cancer.

AS regulation is a major mechanism for the enhancement of transcriptome and proteome diversity, particularly in mammals [36]. A large portion of RBPs cooperate to control this process and are ultimately processed into different mature RNA isoforms. Aberrant expression of RBPs could greatly alter the AS profile in cells and lead to disease or dysplasia [37]. As a canonical splicing factor, TRA2B has recognized AS regulatory functions from insects to mammals. TRA2B promotes HIV-1 RNA processing by directly binding to target RNAs [38]. Higher expression levels of TRA2B were observed in several cancers, including lung, ovary, cervix, stomach, head, and neck cancers, and were associated with neoplasia and metastasis [39]. To uncover the underlying mechanisms, we analyzed the profile of TRA2B RASEs. Based on the results for TRA2B RASEs in TCGA OV transcriptome data, we found that TRA2B has the potential to regulate the cell cycle by influencing the AS pattern of related genes, expanding the knowledge molecular mechanisms of TRA2B in tumor development. We also found that TRA2B repressed the expression of genes associated with cell adhesion, suggesting that TRA2B contributes to cancer cell metastasis by changing the extracellular matrix composition. We validated the AS regulatory functions of

TRA2B in OV patients and cancer cells. We discovered that mitotic cell cycle-related genes were significantly enriched in RASGs of TRA2B, providing an explanation for how TRA2B promotes cell proliferation in cancer. Previous studies suggested that TRA2B regulates the cell cycle by controlling a cassette exon in the NASP gene [21, 24]. We identified several other genes controlling the cell cycle whose AS was regulated by TRA2B, including SMAD4, DSN1, MCM8, and UBE2I. Interestingly, TRA2B knockdown also significantly influenced the AS pattern of TRA2B itself (Fig. 6A), implying that there is a feedback regulatory loop involving TRA2B and its RNAs in cancer cells. These results together demonstrated the novel functional pathways of TRA2B in regulating the cell cycle in cancers.

Although RBPs primarily bind to RNA to regulate AS or the stability of RNAs, RBPs pervasively interact with DNA to regulate gene expression [40]. We then analyzed the regulatory effects of changes in TRA2B expression in HeLa cells, which revealed approximately four hundred DEGs between TRA2B knockdown and control cells. Functional analysis of these DEGs demonstrated their close relationship with cancer development. Most studies of the identified expression regulation of TRA2B were associated with its AS regulatory functions. Based on this concept, there should be a large number of DEGs that are also regulated at the AS level. However, we found that only six genes were regulated by TRA2B at both the expression and AS levels. These results strongly suggest that TRA2B regulates gene expression via other important and undiscovered mechanisms. TRA2B has been reported to regulate gene expression by performing competing RNA or protein roles [41]. TRA2B could also indirectly regulate gene expression by affecting the AS of genes with transcriptional regulation functions. In this study, we found that several genes, including transcription factors (TFs), were regulated by TRA2B at the AS level. Their abnormal transcripts may encode nonfunctional proteins and thus cannot normally regulate the transcription of downstream genes. From our results, the very small overlap between DEGs and RASGs supports our hypothesis that the TRA2B regulatory functions of gene expression and AS do not simultaneously occur for the same gene. A regulatory axis between AS regulation and gene expression regulation could exist, but it needs further investigation.

Conclusions

We used a series of experiments to confirm that the proliferation, apoptosis and invasiveness of epithelial OV cells can be significantly affected by interfering with the expression of TRA2B in tumor cells. On the other hand, TCGA transcriptome analysis revealed that TRA2B plays an important regulatory role and has an oncogenic function in OV development. Survival curves showed that the OS time of patients was correlated with the expression level of genes that were regulated by TRA2B in OV. Therefore, the abnormal regulation of AS by TRA2B plays a vital role in the development of OV. Of course, there are some limitations to this experiment. At present, experiments with animals and clinical specimens are being performed to further verify these findings to confirm the role of TRA2B as an RNA binding protein that affects AS in the pathogenesis of OV and to determine its clinical significance as a drug target.

Materials And Methods

Cell culture and transfections

The human cervical carcinoma (CC) cell line HeLa (CCTCC@GDC0009) was obtained from the China Center for Type Culture Collection (Wuhan, Hubei, China). The human OV cell lines HO8910 and A2780 were obtained from the American Type Culture Collection (Rockville, MD, USA). HeLa, HO8910 and A2780 cells were cultured in Dulbecco's modified Eagle's medium (DMEM) with 10% fetal bovine serum (FBS), 100 μg/mL streptomycin, and 100 U/mL penicillin at 37°C in 5% CO_2. Plasmid transfection of HeLa cells was performed using Lipofectamine 2000 (Invitrogen, Carlsbad, CA, USA) according to the manufacturer's protocol. Transfected cells were harvested after 48 h for RT-qPCR analysis. The efficient *TRA2B* short hairpin RNA (shRNA) sequence was 5'-TACTCACCTCGTCGCTATTAA-3'; The siRNA sequences were as follows: TRA2B siRNA 405 sense: 5'-GGUCUUACAGUCGAGAUUATT-3', antisense: 5'-UAAUCUCGACUGUAAGACCTT-3'; TRA2B siRNA 581 sense: 5'-CCCAUUGCCGAUGUGUCUATT-3', antisense: 5'-UAGACACAUCGGCAAUGGGTT-3'; TRA2B siRNA 798 sense: 5'-GCUCUCGCCGUCGGGAUUATT-3', antisense: 5'-UAAUCCCGACGGCGAGAGCTT-3'; and siRNA NC (negative control) sense: 5'-UUCUCCGAACGUGUCACGUTT-3', antisense: 5'-ACGUGACACGUUCGGAGAATT-3'.

Assessment of the effects of knockdown by shRNA

Glyceraldehyde-3-phosphate dehydrogenase (GAPDH) was used as a control gene to assess the effects of *TRA2B* knockdown. cDNA synthesis was performed using standard procedures, and RT-qPCR was performed on a Bio-Rad S1000 with Bestar SYBR Green RT-PCR Master Mix (DBI Bioscience, Shanghai, China). The level of each transcript was then normalized to the GAPDH mRNA level using the $2^{-\Delta\Delta}$CT method [42]. Comparisons were performed with a paired Student's t-test using GraphPad Prism software (San Diego, CA, USA). The sequences of primers were as follows: TRA2B forward: 5'-TTATACCCGGTCACGGTCTC-3', reverse: 5'-AGCTCAGCCCAAATACTCCA-3'; CYR61 forward: 5'-ACCCTCGGCTGGTCAAAGT-3', reverse: 5'-GCTTCAGTGAGCTGCCTTTT-3'; CTGF forward: 5'-ACAGGCGGCTCTGCTTCTC-3', reverse: 5'-GGCCCAGACCCAACTATGA-3'; FN1 forward: 5'-CACTCATCTCCAACGGCATAA-3', reverse: 5'-GGCTTGAACCAACCTACGG-3'; and HMGA2 forward: 5'-CCTCTGCGACCTCAAAGCC-3', reverse: 5'-CGCTGCCACCATCAACACC-3'.

Cell proliferation assay

The MTT assay was used to assess cell proliferation. Briefly, HeLa cells were cultured in 96-well plates and then transfected with the vector using Lipofectamine 2000 (Invitrogen) according to the manufacturer's protocol. The cells were then incubated at 37°C for 48 h. Subsequently, MTT solution (5 mg/mL [0.025 mL]) was added to each well, and the cells were incubated for another 4 h. After centrifugation, the supernatant was removed from each well. The colored formazan crystals produced from MTT in each well were dissolved in DMSO (0.15 mL), and the optical density (OD) was measured at 490 nm. The cytotoxic effects of TRA2B shRNA were determined using the Cell Counting Kit-8 (CCK-8) assay. Cells were cultured in 96-well plates at a density of 104/well and incubated overnight at 37°C with 5% CO_2. TRA2B shRNA, TRA2B siRNA 405, TRA2B siRNA 581 and TRA2B siRNA 798 were added to 96-well plates in triplicate and incubated for 0 h, 12 h, 24 h, 48 h, or 72 h. Then, 10 μl of the CCK-8 solution

was added to each well and incubated for 2 h at 37°C with 5% CO_2, according to the manufacturer's protocol (Dojindo, Japan).

Flow cytometric analysis of cell apoptosis

HeLa, HO8910 and A2780 cells were seeded in 24-well culture plates. When the cells reached 70% confluence, they were transfected with the vector using Lipofectamine 2000 according to the manufacturer's protocol. The cells were then incubated at 37°C for 48 h, and viable cells were harvested and washed twice with phosphate-buffered saline (PBS). Viable cells were double-stained with fluorescein isothiocyanate (FITC)-conjugated annexin V and 7-amino actinomycin D (7-AAD; Biotech Co., Ltd., Suzhou, Jiangsu, China). The percentage of cell apoptosis was defined as the sum of the right lower and upper quadrants. The induction of apoptosis was detected using an annexin V/PI apoptosis detection kit (Nanjing Key Gen Biotech Co, Jiangsu, China) according to the manufacturer's instructions. Briefly, the cells were cultured at a density of 1.0×10^5 cells/mL, treated with TRA2B shRNA/TRA2B siRNA and cultured for 12 h at 37℃ with 5% CO_2. All samples were analyzed using a FACSort Flow Cytometer (Becton Dickinson, USA).

Western blotting analysis

Protein extracts were generated from HO8910 and A2780 cells cultivated for 30 min in a 37℃ atmosphere containing 5% CO_2. The extracts were separated using SDS polyacrylamide gel electrophoresis and electrophoretically transferred to nitrocellulose membranes (Millipore, USA). Standard Western blot analyses were performed using antibodies against CTGF, CYR61, FN1, HMGA2, ASAP3, ERBB3, IL-6, IL-1, JUN, MAP2K8, MMP13, NPNT, ODC1 VEGFC and GAPDH (Santa Cruz, CA, USA). Immunoreactive proteins were visualized using goat anti-rabbit secondary antibody-HRP conjugate (Santa Cruz, CA, USA) and detected through enhanced chemiluminescence. BandScan software was used to analyze the grayscale value.

Scratch migration assay

HO8910 and A2780 cells (2×10^5) were seeded in 6-well culture plates. Confluent monolayers were scraped. Plates were washed twice to remove detached cells and incubated in growth medium. After 0 h or 24 h, cell migration was photographed, and the newly covered area was measured with ImageJ software.

Transwell assay

To explore whether TRA2B could influence the invasive ability of OV cells, a Transwell assay was performed. The upper chamber was covered with 100 μl Matrigel (1 mg/ml) (BD, USA). After the Matrigel formed a gel, 200 μl of cell suspension was added to the upper Transwell chamber and cultured for 24 h at 37℃. Then, cells on the upper chamber were removed, and cells from the lower surface were fixed with 7% ice ethanol and stained with 0.5% crystal violet for 30 min. The cells were counted by ImagePro Plus.

RNA extraction and sequencing

The HeLa cells were ground into fine powder before RNA extraction. Total RNA was extracted with TRIzol (Ambion, Shanghai, China). The RNA was further purified with two phenol-chloroform treatments and then treated with RQ1 DNase (Promega, Madison, WI, USA) to remove DNA. The quality and quantity of the purified RNA were redetermined by measuring the absorbance at 260 nm/280 nm (A260/A280) using SmartSpec Plus (BioRad, Hercules, California, USA). The integrity of RNA was further verified by 1.5% agarose gel electrophoresis.

For each sample, 1 μg of the total RNA was used for RNA-seq library preparation using the VAHTS Stranded mRNA-seq Library Prep Kit (Vazyme, Nanjing, Jiangsu, China). Polyadenylated mRNAs were purified and fragmented and then converted into double-stranded cDNA. After end repair and A tailing, the DNAs were ligated to VAHTS RNA Adapters (Vazyme). Purified ligation products corresponding to 200–500 bp were digested with heat-labile uracil-DNA glycosylase (UDG), and the single-stranded cDNA was amplified, purified, quantified, and stored at -80°C before sequencing.

For high-throughput sequencing, the libraries were prepared following the manufacturer's instructions and applied to the Illumina HiSeq X Ten system for 150 nt paired-end sequencing.

RNA-seq raw data processing and alignment

Raw reads containing more than 2-N bases were first discarded. Then, adaptors and low-quality bases were trimmed from raw sequencing reads using FASTX-Toolkit (version 0.0.13). Short reads less than 16 nt were also excluded. The clean reads were then aligned to the GRch38 genome by TopHat2 [43], allowing 4 mismatches. Uniquely mapped reads were used for gene read number counting and fragments per kilobase of transcript per million fragments mapped (FPKM) calculation [44].

Differentially expressed gene (DEG) analysis

The R Bioconductor packages edgeR [45] and DESeq [46] were utilized to screen out the DEGs. FDR < 0.05 and fold change (FC) > 2 or < 0.5 were set as the cutoff criteria for identifying DEGs.

AS analysis

The alternative splicing events (ASEs) and RASEs between the samples were defined and quantified using the ABLas pipeline, as described previously [47, 48]. In brief, ABLas detection of 10 types of ASEs was based on splice junction reads, including exon skipping (ES), alternative 5' splice site (A5SS), alternative 3' splice site (A3SS), intron retention (IR), mutually exclusive exons (MXEs), mutually exclusive 5' UTRs (5pMXEs), mutually exclusive 3' UTRs (3pMXEs), cassette exon, A3SS&ES, and A5SS&ES.

To assess RBP RASEs, Student's *t*-test was used to evaluate the significance of the ratio alteration of ASEs. Those events that were significant at the P value cutoff corresponding to a false discovery rate cutoff of 5% were considered RBP RASEs.

Functional enrichment analys

To sort out functional categories of DEGs, the enriched gene ontology (GO) terms and Kyoto Encyclopedia of Genes and Genomes (KEGG) pathways were identified using the KOBAS 2.0 server [49]. The hypergeometric test and Benjamin-Hochberg false discovery rate (FDR) controlling procedure were used to define the enrichment of each term.

The Kaplan-Meier (KM) plotter analysis

The prognostic significance of the mRNA expression of AS-regulated genes in OV was evaluated using KM plotter (www.kmplot.com), an online database including microarray gene expression data and survival information, which contains gene expression data and survival information for 1,657 clinical OV patients [50].

Declarations

Ethical approval and consent to participate

This article does not contain any studies with human participants or animals performed by any of the authors.

Consent for publication

All authors have approved the content of the manuscript.

Availability of data and materials

RNA-seq data in this publication have been deposited in NCBI's Gene Expression Omnibus and are accessible through GEO series accession number GSE176214. Other data are available from the corresponding author.

Competing interests

All authors declare no competing interests in this study.

Funding

This work was supported by the National Natural Science Foundation of China (81572563) and the National Science Foundations of HUBEI (2018CFB235). The funder had role in study design, data collection and analysis, decision to publish, or preparation of the manuscript.

Authors' contributions

Ting Zhou, Shixuan Wang, Ronghua Liu conceived the project, designed and supervised the Experiments. Ting Zhou, Peiying Fu and Dong Chen performed the experiment. Ting Zhou, Peiying Fu, Shixuan Wang, Ronghua Liu analyzed the data. Ting Zhou, Shixuan Wang drafted the manuscript. All authors reviewed the draft manuscript and approved the final version of the manuscript.

Acknowledgements

We are very thankful Dr. Yi Zhang's team members for helpful discussions.

References

1. Jayson GC, Kohn EC, Kitchener HC, Ledermann JA. Ovarian cancer. The Lancet. 2014; 384:1376-1388.
2. Shih Ie M, Kurman RJ. Ovarian tumorigenesis: a proposed model based on morphological and molecular genetic analysis. Am J Pathol. 2004;164:1511-1518.
3. Hentze MW, Castello A, Schwarzl T, Preiss T. A. brave new world of RNA-binding proteins. Nat Rev Mol Cell Biol. 2018;19:327-341.
4. Gerstberger S, Hafner M, Tuschl T. A census of human RNA-binding proteins. Nature reviews Genetics. 2014;15:829-845.
5. Pereira B, Billaud M, Almeida R. RNA-Binding Proteins in Cancer: Old Players and New Actors. Trends Cancer. 2017;3:506-528.
6. Nayler O, Cap C, Stamm S. Human transformer-2-beta gene (SFRS10): complete nucleotide sequence, chromosomal localization, and generation of a tissue-specific isoform. Genomics. 1998;53:191-202.
7. Verhulst EC, van de Zande L, Beukeboom LW Insect sex determination: it all evolves around transformer. Curr Opin Genet Dev. 2010;20:376-383.
8. Nissen I, Muller M, Beye M. The Am-tra2 gene is an essential regulator of female splice regulation at two levels of the sex determination hierarchy of the honeybee. Genetics. 2012;192:1015-1026.
9. Dauwalder B, Amaya-Manzanares F, Mattox W. A human homologue of the Drosophila sex determination factor transformer-2 has conserved splicing regulatory functions. Proc Natl Acad Sci U S A.1996;93:9004-9009.
10. Jamros MA, Aubol BE, Keshwani MM, Zhang Z, Stamm S, Adams JA. Intra-domain Cross-talk Regulates Serine-arginine Protein Kinase 1-dependent Phosphorylation and Splicing Function of Transformer 2beta1. J Biol Chem.2015;290:17269-17281.
11. Li SJ, Qi Y, Zhao JJ, Li Y, Liu XY, Chen XH, et al. Characterization of nuclear localization signals (NLSs) and function of NLSs and phosphorylation of serine residues in subcellular and subnuclear localization of transformer-2beta (Tra2beta). J Biol Chem. 2013;288:8898-8909.
12. Shukla JN, Palli SR. Tribolium castaneum Transformer-2 regulates sex determination and development in both males and females. Insect Biochem Mol Biol. 2013;43:1125-1132.
13. Mikoluk C, Nagengast AA, DiAngelo JR. The splicing factor transformer2 (tra2) functions in the Drosophila fat body to regulate lipid storage. Biochem Biophys Res Commun. 2018;495:1528-1533.
14. Patel RS, Carter G, Cooper DR, Apostolatos H, Patel NA. Transformer 2beta homolog (Drosophila) (TRA2B) regulates protein kinase C deltaI (PKCdeltaI) splice variant expression during 3T3L1 preadipocyte cell cycle. J Biol Chem. 2014;289: 31662-31672.

15. Li X, Jin B, Dong Y, Chen X, Tu Z, Gu J. Two of the three Transformer-2 genes are required for ovarian development in Aedes albopictus. Insect Biochem Mol Biol. 2019;109:92-105.
16. Zheng X, Reho JJ, Wirth B, Fisher SA. TRA2beta controls Mypt1 exon 24 splicing in the developmental maturation of mouse mesenteric artery smooth muscle. Am J Physiol Cell Physiol. 2015;308:C289-296.
17. Best A, James K, Dalgliesh C, Hong E, Kheirolahi-Kouhestani M, Curk T, et al. Human Tra2 proteins jointly control a CHEK1 splicing switch among alternative and constitutive target exons. Nat Commun. 2014;5:4760.
18. Paudel D, Ouyang Y, Huang Q, Zhou W, Wang J, Poorekhorsandi ME, et al. Expression of TRA2B in endometrial carcinoma and its regulatory roles in endometrial carcinoma cells. Oncol Lett. 2019;182:455-2463.
19. Kuwano Y, Nishida K, Kajita K, Satake Y, Akaike Y, Fujita K, et al. Transformer 2beta and miR-204 regulate apoptosis through competitive binding to 3' UTR of BCL2 mRNA. Cell Death Differ. 2015;22:815-825.
20. Best A, Dagliesh C, Ehrmann I, Kheirollahi-Kouhestani M, Tyson-Capper A, Elliott DJ. Expression of Tra2 beta in Cancer Cells as a Potential Contributory Factor to Neoplasia and Metastasis. Int J Cell Biol. 2013;2013:843781.
21. Watermann DO, Tang Y, Zur Hausen A, Jager M, Stamm S, Stickeler E. Splicing factor Tra2-beta1 is specifically induced in breast cancer and regulates alternative splicing of the CD44 gene. Cancer Res. 2006;66:4774-4780.
22. Venables JP, Bourgeois CF, Dalgliesh C, Kister L, Stevenin J, Elliott DJ. Up-regulation of the ubiquitous alternative splicing factor Tra2beta causes inclusion of a germ cell-specific exon. Hum Mol Genet. 2005;14:2289-2303.
23. Grellscheid S, Dalgliesh C, Storbeck M, Best A, Liu Y, Jakubik M, et al. Identification of evolutionarily conserved exons as regulated targets for the splicing activator tra2beta in development. PLoS Genet. 2011;7:e1002390.
24. Fischer DC, Noack K, Runnebaum IB, Watermann DO, Kieback DG, Stamm S, et al. Expression of splicing factors in human ovarian cancer. Oncol Rep. 2004;11:1085-1090.
25. Hirschfeld M, Jaeger M, Buratti E, Stuani C, Grueneisen J, Gitsch G, et al. Expression of tumor-promoting Cyr61 is regulated by hTRA2-beta1 and acidosis. Hum Mol Genet. 2011;20:2356-2365.
26. D'Amico D, Mottis A, Potenza F, Sorrentino V, Li H, Romani M, et al. The RNA-Binding Protein PUM2 Impairs Mitochondrial Dynamics and Mitophagy During Aging. Mol Cell. 2019;73:775-787.
27. Wilbertz JH, Voigt F, Horvathova I, Roth G, Zhan Y, Chao JA. Single-Molecule Imaging of mRNA Localization and Regulation during the Integrated Stress Response. Mol Cell. 2019;73:946-958.
28. Liu Y, Mi Y, Mueller T, Kreibich S, Williams EG, Van Drogen A, et al. Multi-omic measurements of heterogeneity in HeLa cells across laboratories. Nat Biotechnol. 2019;37:314-322.
29. Masters JR.HeLa cells 50 years on: the good, the bad and the ugly. Nat Rev Cancer. 2002;2:315-319.

30. Dang CV. Links between metabolism and cancer. Genes Dev. 2012;26:877-890.
31. Hanahan D, Weinberg RA. Hallmarks of cancer: the next generation. Cell. 2011;144:646-674.
32. Xia H, Chen D, Wu Q, Wu G, Zhou Y, Zhang Y, et al.CELF1 preferentially binds to exon-intron boundary and regulates alternative splicing in HeLa cells. Biochim Biophys Acta. 2017;1860:911-921.
33. Dhar A, Ray A.The CCN family proteins in carcinogenesis. Exp Oncol. 2010;3: 22-29.
34. Xie D, Yin D, Wang HJ, Liu GT, Elashoff R, Black K, et al. Levels of expression of CYR61 and CTGF are prognostic for tumor progression and survival of individuals with gliomas. Clin Cancer Res. 2004;10:2072-2081.
35. Fischer DC, Noack K, Runnebaum IB, Watermann DO, Kieback DG, Stamm S, et al. Expression of splicing factors in human ovarian cancer. Oncol Rep. 2004; 11:1085-1090.
36. Keren H, Lev-Maor G, Ast G. Alternative splicing and evolution: diversification, exon definition and function. Nature reviews Genetics. 2010;11:345-355.
37. Kalsotra A, Cooper TA. Functional consequences of developmentally regulated alternative splicing. Nature reviews Genetics. 2011;12:715-729.
38. Brillen AL, Walotka L, Hillebrand F, Muller L, Widera M, Theiss S, et al. Analysis of Competing HIV-1 Splice Donor Sites Uncovers a Tight Cluster of Splicing Regulatory Elements within Exon 2/2b. J Virol. 2017;91:e00389-17.
39. Best A, Dagliesh C, Ehrmann I, Kheirollahi-Kouhestani M, Tyson-Capper A, Elliott DJ. Expression of Tra2β in Cancer Cells as a Potential Contributory Factor to Neoplasia and Metastasis. Int J Cell Biol. 2013;2013:843781.
40. Xiao R, Chen JY, Liang Z, Luo D, Chen G, Lu ZJ, et al (2019) Pervasive Chromatin-RNA Binding Protein Interactions Enable RNA-Based Regulation of Transcription. Cell 178, 107-121
41. Kajita K, Kuwano Y, Satake Y, Kano S, Kurokawa K, Akaike Y, et al. Ultraconserved region-containing Transformer 2beta4 controls senescence of colon cancer cells. Oncogenesis. 2016;5:e213.
42. Livak KJ, Schmittgen TD.Analysis of relative gene expression data using real-time quantitative PCR and the 2(-Delta Delta C(T)) Method. Methods. 2001;25:402-408.
43. Kim D, Pertea G, Trapnell C, Pimentel H, Kelley R, Salzberg SL. TopHat2: accurate alignment of transcriptomes in the presence of insertions, deletions and gene fusions. Genome Biology. 2013;14:R36.
44. Trapnell C, Williams BA, Pertea G, Mortazavi A, Kwan G, van Baren MJ, et al.Transcript assembly and quantification by RNA-Seq reveals unannotated transcripts and isoform switching during cell differentiation. Nat Biotechnol. 2010;28:511-515.
45. Robinson MD, McCarthy DJ, Smyth GK. edgeR: a Bioconductor package for differential expression analysis of digital gene expression data. Bioinformatics. 2010; 26:139-140.
46. Anders S, Huber W. Differential expression analysis for sequence count data. Genome Biol. 2010;11:R106.

47. Xia H, Dong C, Wu Q, Gang W, Zhou Y, Yi Z, et al. CELF1 preferentially binds to exon-intron boundary and regulates alternative splicing in HeLa cells. Biochimica et biophysica acta. 2017;1860:911-921.
48. Jin L, Li G, Yu D, Wei H, Chao C, Liao S, et al. Transcriptome analysis reveals the complexity of alternative splicing regulation in the fungus Verticillium dahliae. Bmc Genomics. 2017;18:130.
49. Xie C, Mao X, Huang J, Ding Y, Wu J, Dong S, et al. KOBAS 2.0: a web server for annotation and identification of enriched pathways and diseases. Nucleic Acids Research. 2011;39:316-322.

Gyorffy B, Lanczky A, Szallasi Z. mplementing an online tool for genome-wide validation of survival-associated biomarkers in ovarian-cancer using microarray data from 1287 patients. Endocr Relat Cancer. 2012;l19:197-208.

Figures

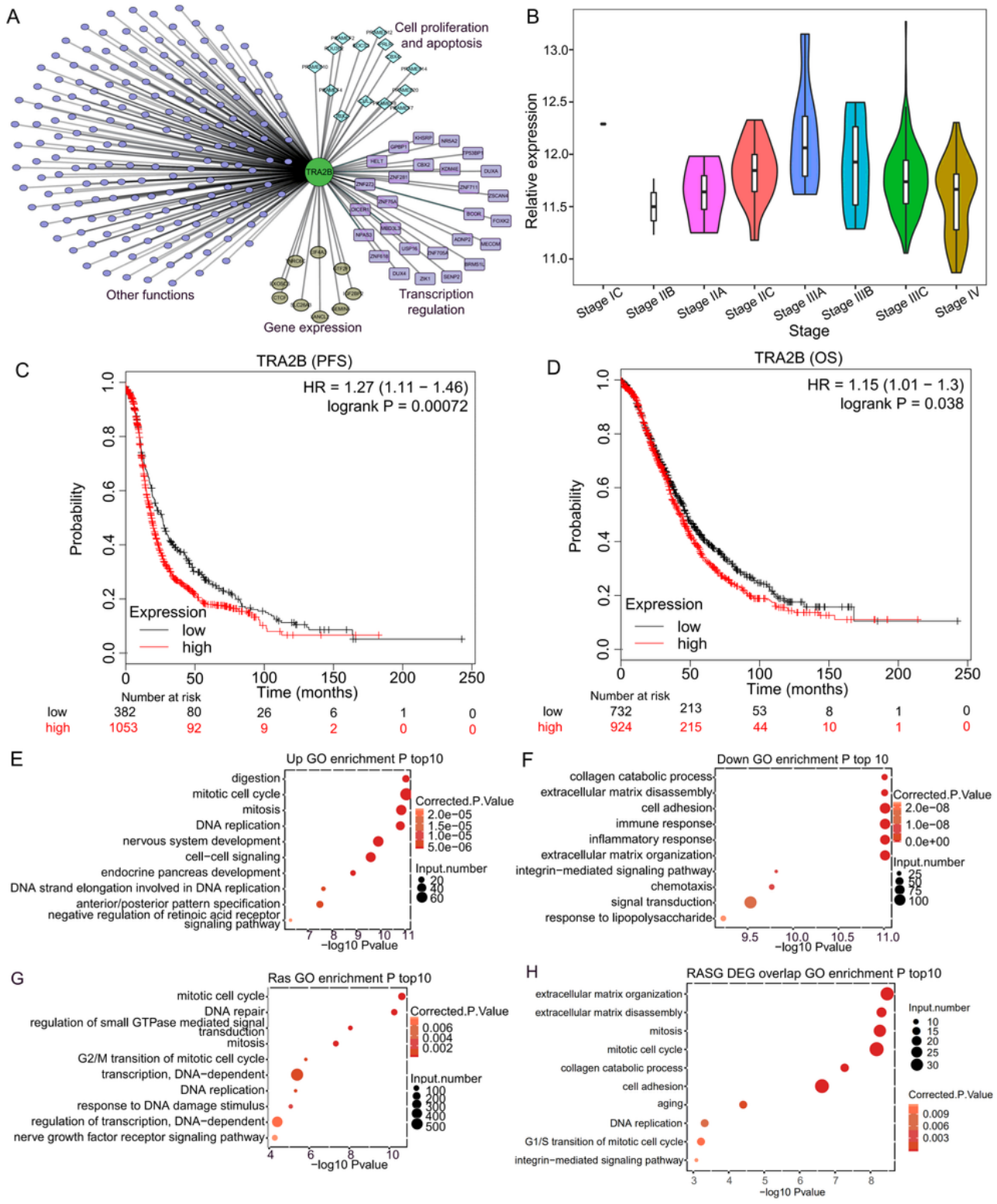

Figure 1

TCGA transcriptome analysis revealed the potential oncogenic function of TRA2B in OV. (A) Violin plot showing the expression pattern of TRA2B during the tumor stages of OV. Only one sample was obtained for stage IC. (B) Coexpression network between TRA2B and its coexpressed genes. Functional clusters of coexpressed genes are labeled. (C, D) Survival analysis (PFS and OS) of TRA2B in OV by KM plotter demonstrated that OV patients with higher TRA2B expression levels globally had shorter survival times

than patients with lower TRA2B expression levels. (E) Bubble plot showing the top 10 enriched GO BP terms for upregulated genes in TRA2B higher expressed patients compared with lower expressed patients. (F) Bubble plot showing the top 10 enriched GO BP terms for downregulated genes in TRA2B-high patients compared with TRA2B-low patients. (G) Bubble plot showing the top 10 enriched GO BP terms for RASGs between TRA2B-high and TRA2B-low patients. (H) Bubble plot showing the top 10 enriched GO BP terms for genes that were both DEGs and RASGs between TRA2B-high and TRA2B-low patients.

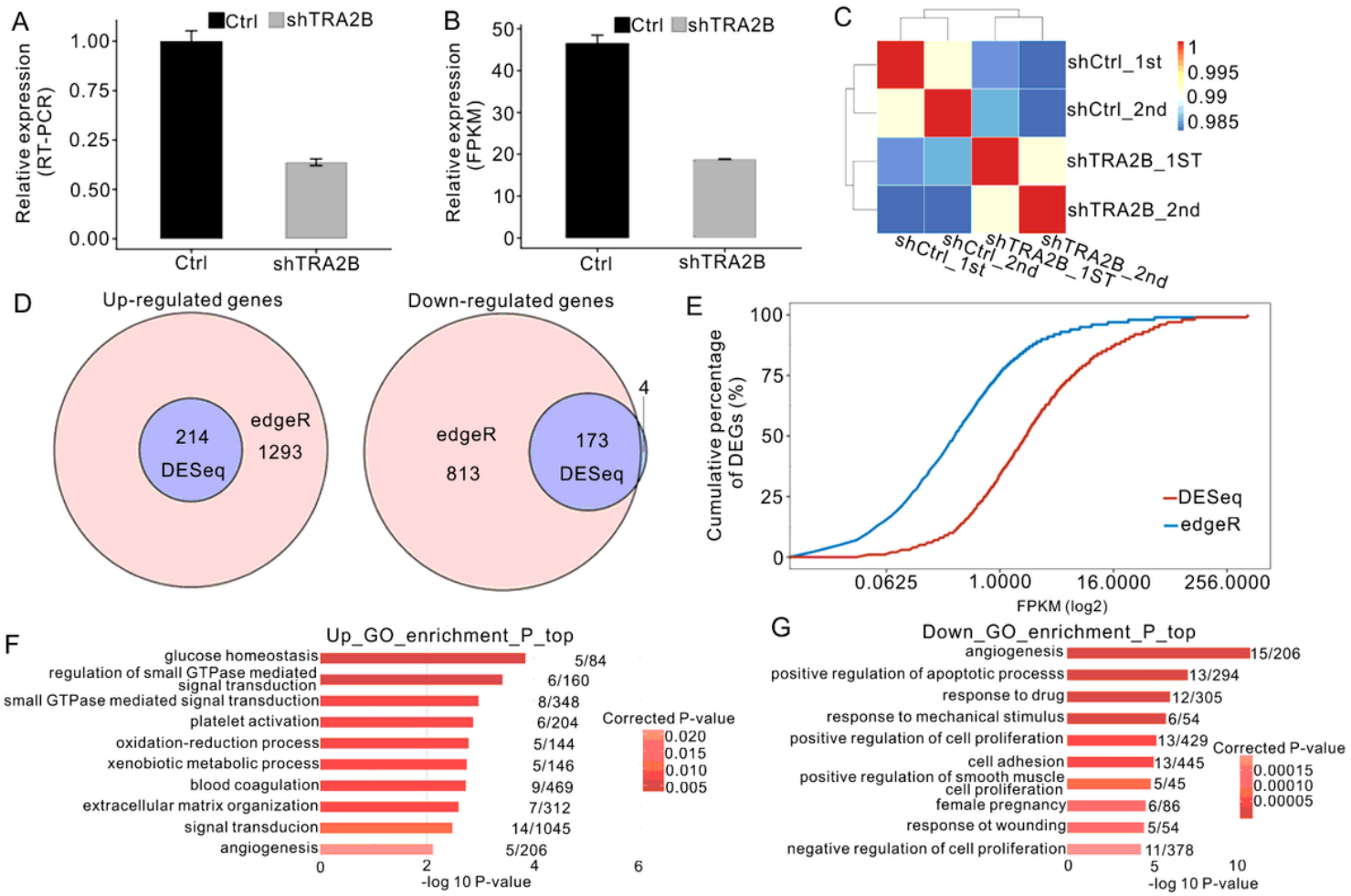

Figure 2

Global RNA-seq profile and the DEGs regulated by TRA2B knockdown. (A-B) Bar plot showing TRA2B mRNA expression in HeLa cells after 48 h of transfection with TRA2B-specific shRNA or control vector, as assessed by RT-qPCR (A), and FPKM values from RNA-seq (B). (C) Heat map showing the Pearson correlation matrix obtained by comparing the control vector- and TRA2B shRNA-treated samples. (D) Venn diagram showing the overlapping DEGs detected by edgeR and DESeq. Upregulated (left panel) and downregulated (right panel) genes are illustrated. (E) Line plot showing the cumulative percentage of DEGs by their FPKM values. (F-G) Bar plot showing the top ten enriched GO BP terms for the upregulated (E) and downregulated (F) genes.

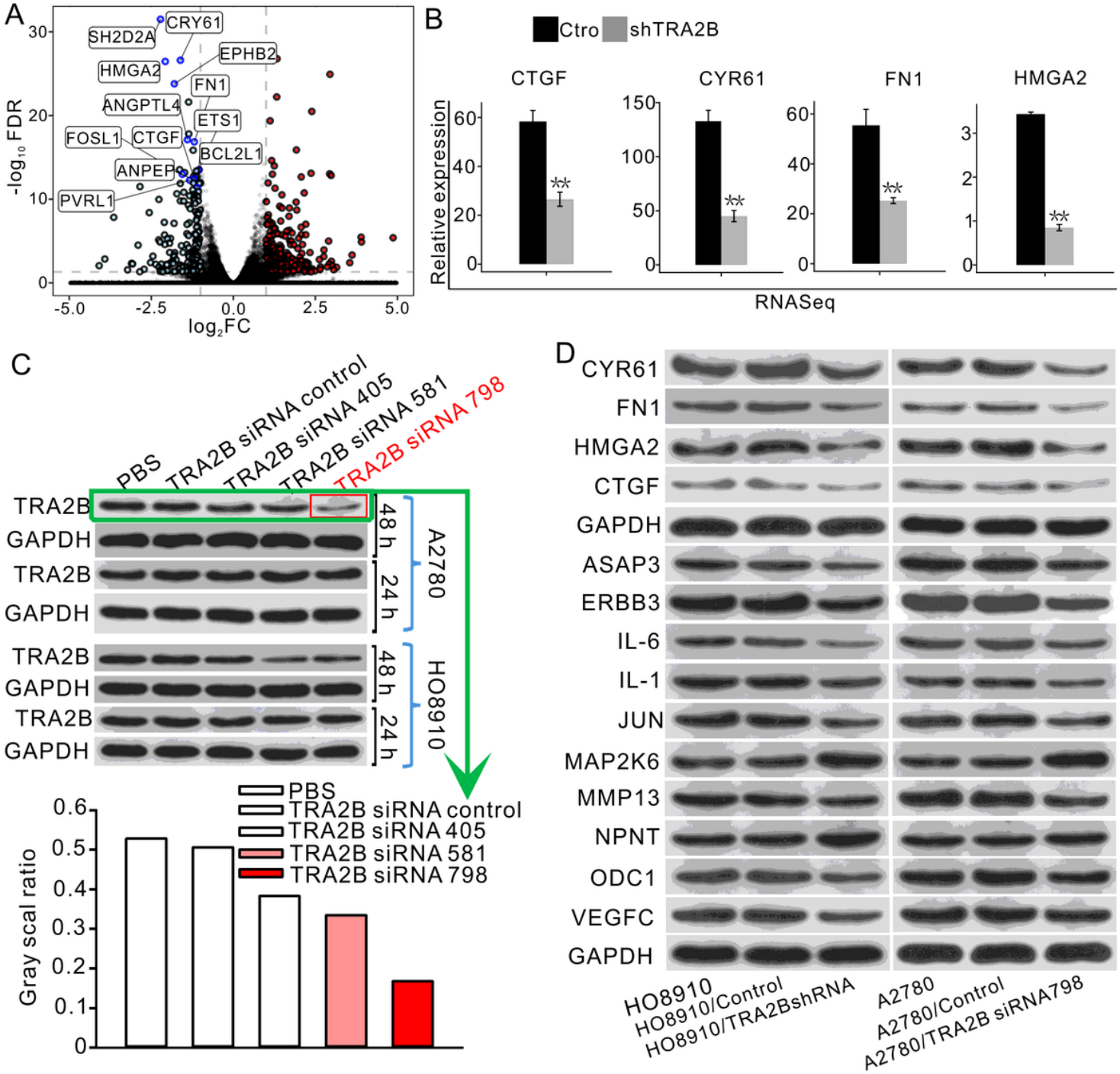

Figure 3

TRA2B significantly represses the expression of angiogenesis- and apoptosis-related genes. (A) Volcano plot showing the genes upregulated and downregulated by TRA2B knockdown. Genes with the top significant FDR values from the top 10 GO BP terms are shown in the figure. (B) Bar plot showing the expression difference between control and TRA2B siRNA samples of selected genes from (A). (C) Screening and validation of the most effective TRA2B siRNA in OV cells. Western blotting and corresponding quantitative results of TRA2B siRNA and shRNA in HO8910 and A2780 OV cell lines. (D) Western blotting and corresponding quantitative results of selected proteins (CYR61, FN1, HMGA2, CTGF,

ASAP3, ERBB3, IL-6, IL-1, JUN, MAP2K6, NPNT, ODC1 and VEGFC) regulated by TRA2B in ovarian cell lines.

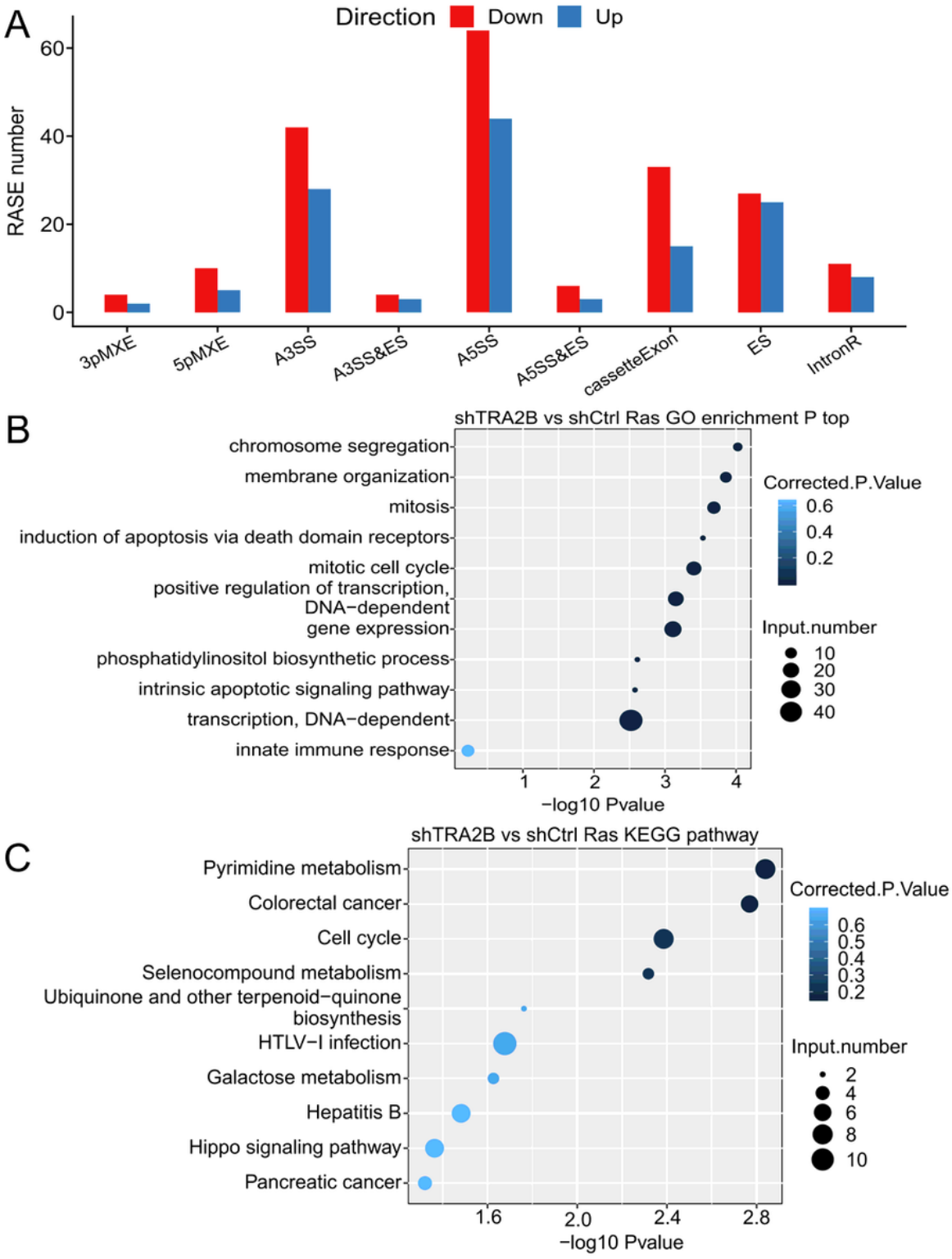

Figure 4

TRA2B regulates AS events in HeLa cells. (A) Bar plot showing the number of RASEs in TRA2B knockdown versus control cells. RASEs are presented by the different AS types. (B) Bar plot showing the

top ten enriched GO BP terms for genes that were regulated at the AS level by TRA2B. (C) Bar plot showing the top ten enriched KEGG pathways for genes that were regulated at the AS level by TRA2B.

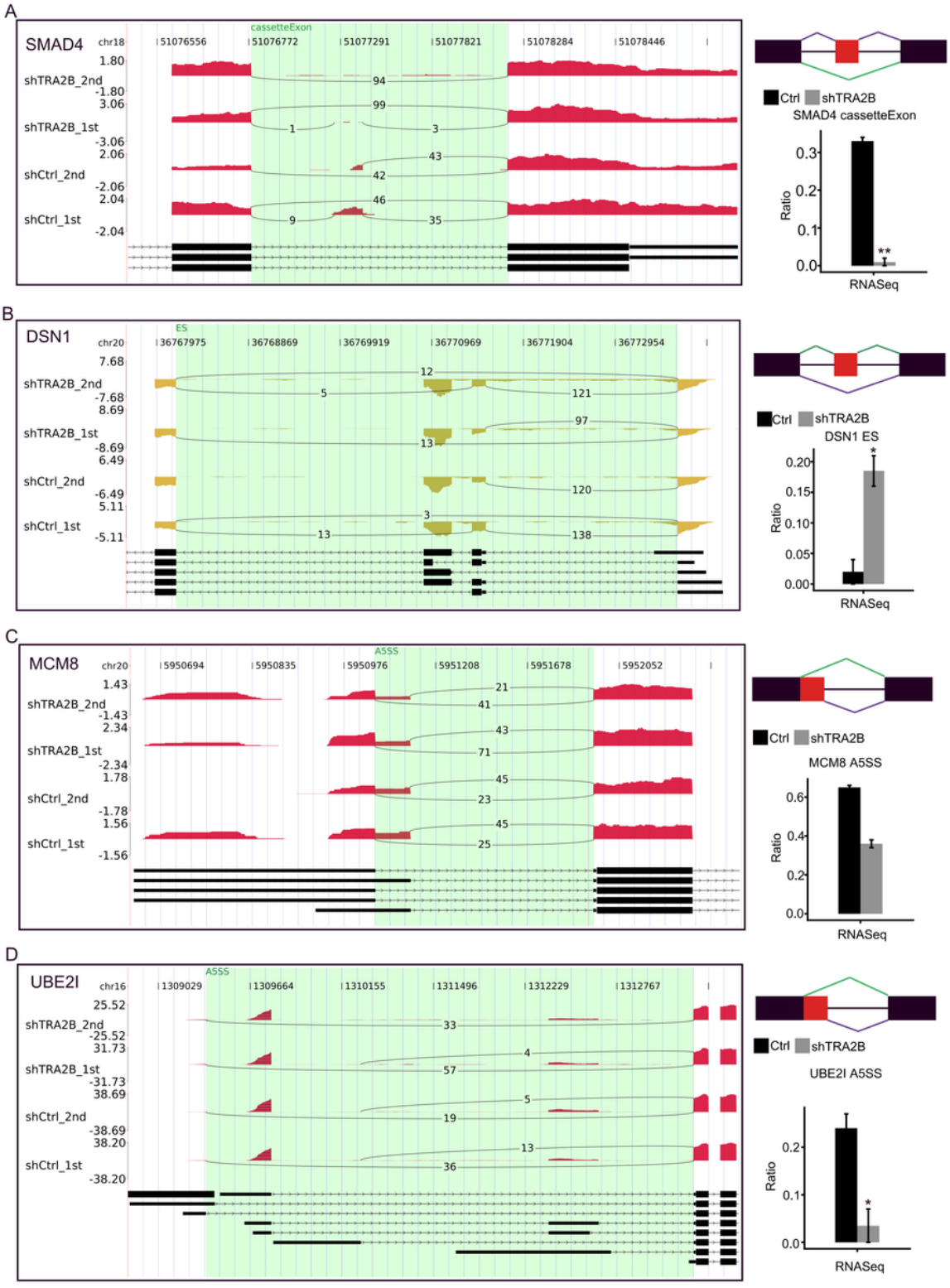

Figure 5

Presentation of TRA2B-affected RASEs. Three RASE genes, SMAD4 (A), DSN1 (B), MCM8 (C) and UBE2I (D), are shown. IGV-Sashimi plots show the AS changes that occurred in control and shTRA2B samples (left panel). The schematic diagrams depict the structures of AS events (right panel, top) AS1 (shown in

purple) and AS2 (shown in green); exon sequences are denoted by boxes, and intron sequences are denoted by the horizontal line. The RNA-seq quantification and statistical significance of RASEs are shown (right panel, bottom). The altered ratio of RASEs was calculated using the formula AS1 junction reads/AS1 junction reads + AS2 junction reads.

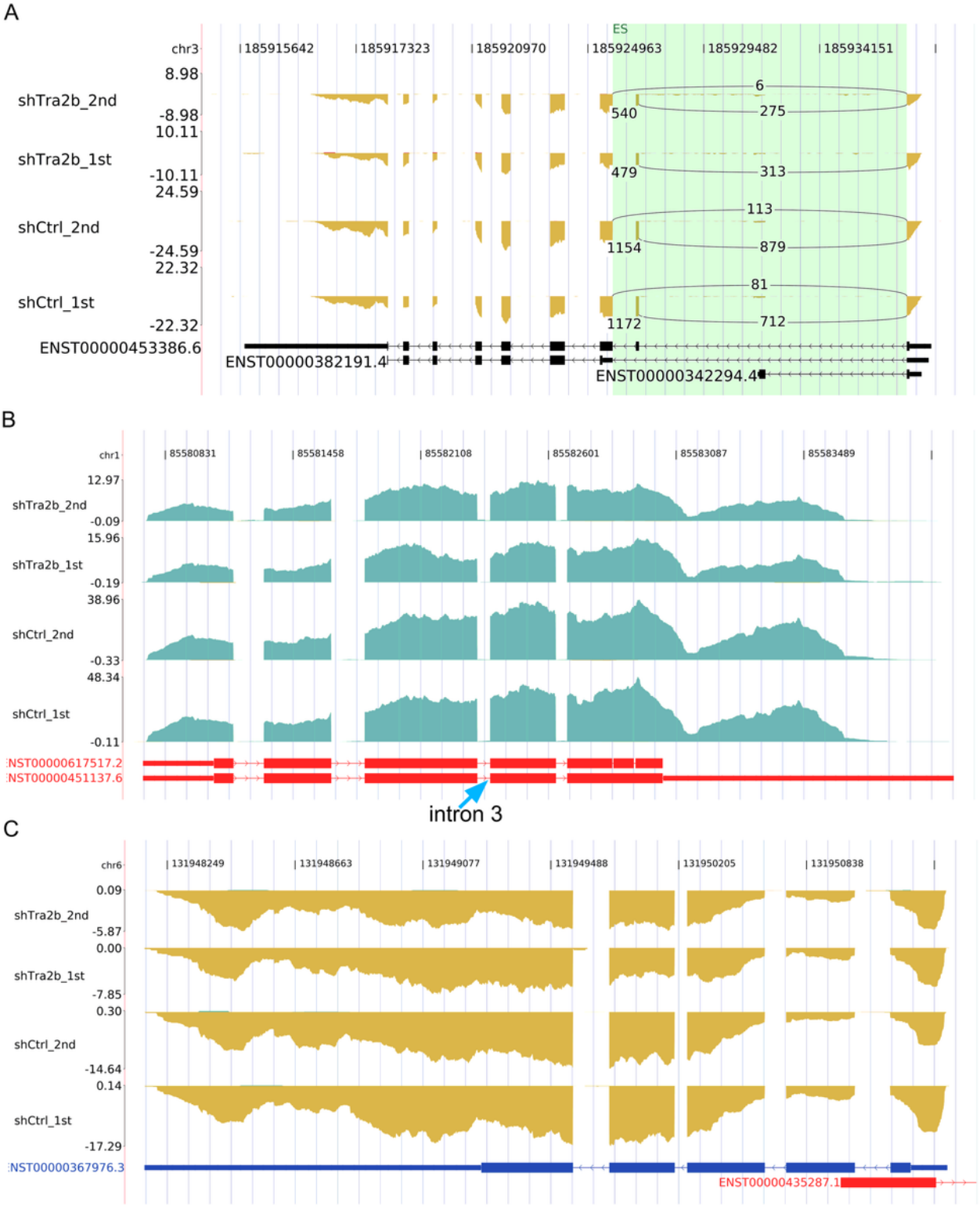

Figure 6

Overlap analysis between DEGs and RASGs in TRA2B knockdown versus control cells. (A) IGV-Sashimi plots show the AS changes and expression level of the TRA2B gene that occurred in control and shTRA2B samples. (B) IGV-Sashimi plots show the AS changes and expression level of the CYR61 gene that occurred in control and shTRA2B samples. (C) IGV-Sashimi plots show the AS changes and expression level of the CTGF gene that occurred in control and shTRA2B samples.

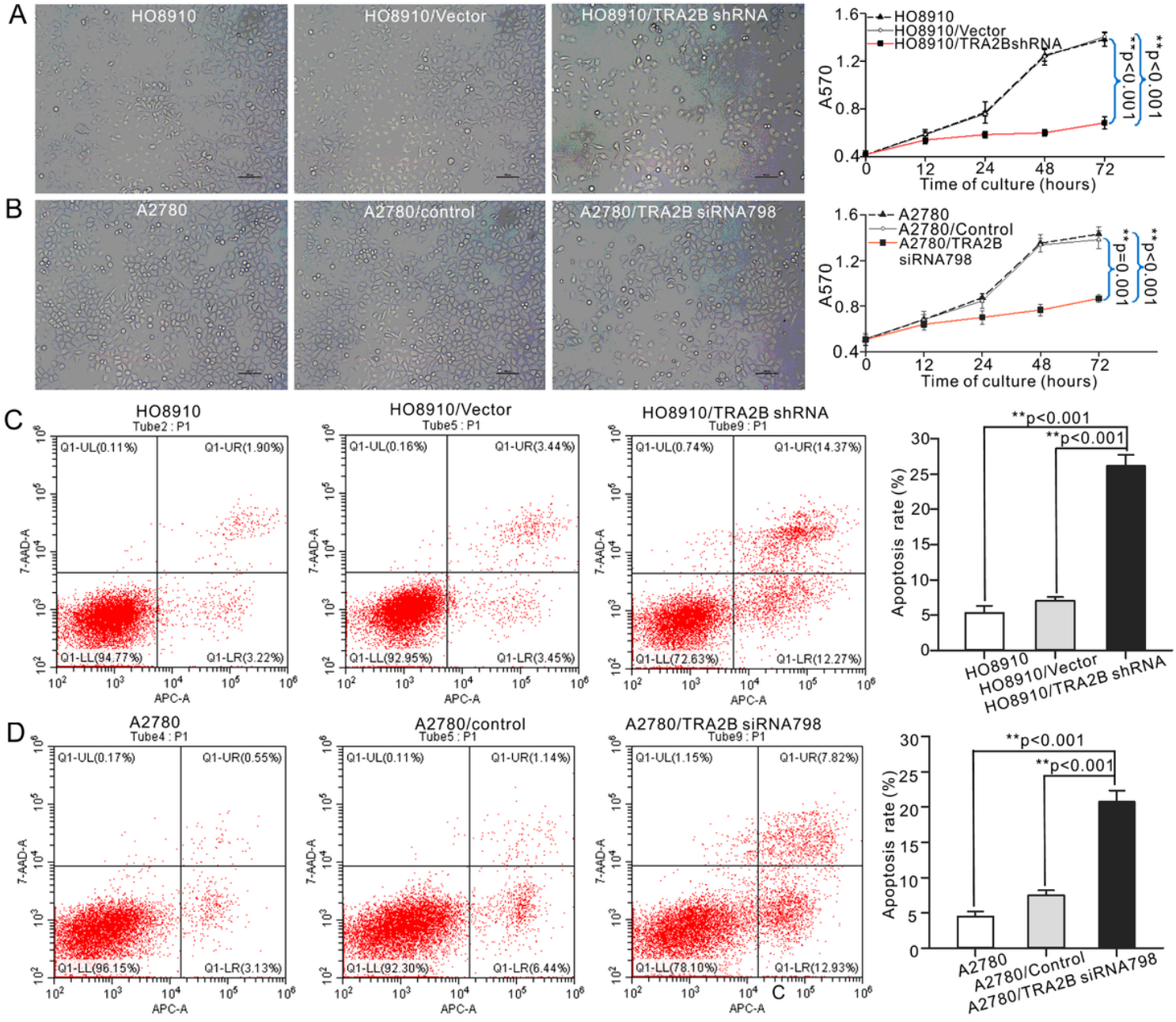

Figure 7

Effects of TRA2B knockdown on the proliferation and apoptosis of OV cells. Cell apoptotic rates in HO8910 and A2780 cell lines were measured using an annexin V/PI apoptosis assay. (A) HO8910 cells were incubated with TRA2B shRNA, vector, or PBS for 48 h. (B). A2780 cells were incubated with TRA2B siRNA 798, control or PBS for 48 h. The standard errors were calculated from three experiments and plotted. (C) HO8910 cells were incubated with TRA2B shRNA, vector, or PBS for 0 h, 12 h, 24 h, 48 h or 72

h. Cell viability levels were assessed under a microscope (right panel). (D). A2780 cells were incubated with TRA2B siRNA 798, control or PBS for 0 h, 12 h, 24 h, 48 h and 72 h. Scale bars, 100 μm. The standard errors were calculated and plotted (left panel). One-way analysis of variance (ANOVA) was performed to assess statistical significance: *, p<0.05; **, p<0.01.

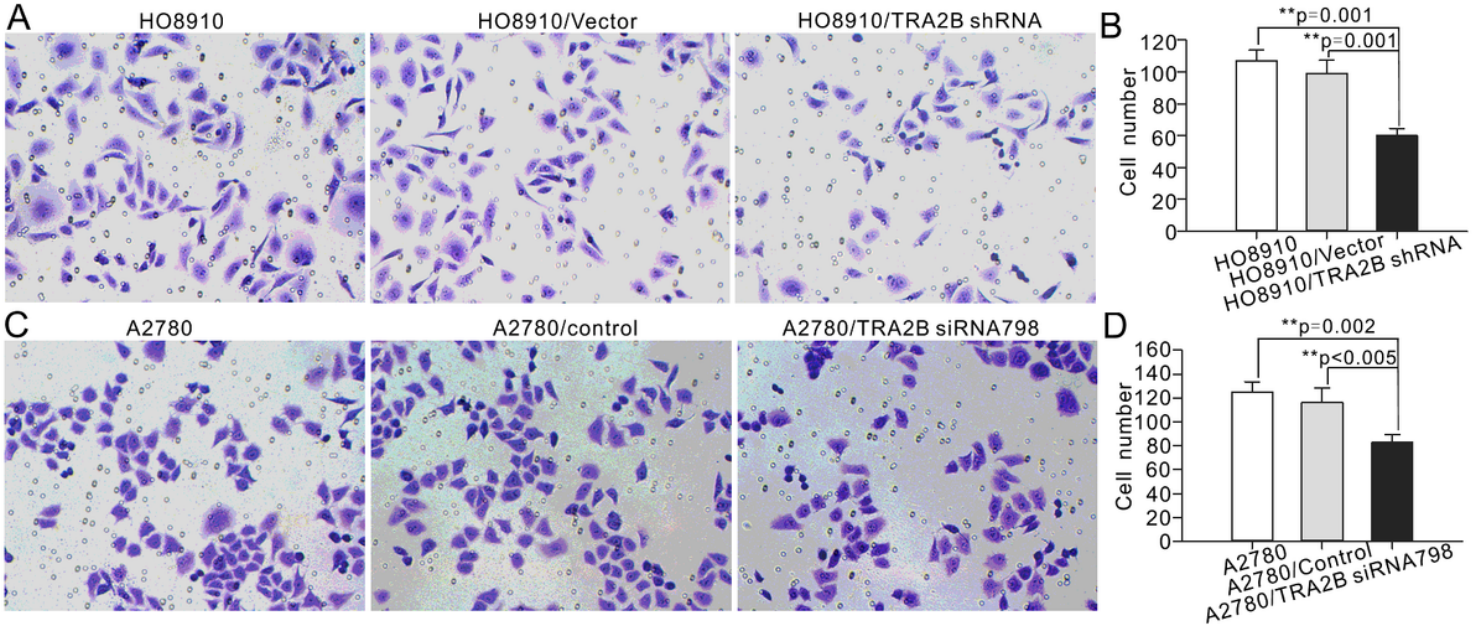

Figure 8

Effects of TRA2B knockdown on the migration of OV cells. A migration assay was performed with HO8910 and A2780 cells. (A) HO8910 cells were incubated with TRA2B shRNA, vector, or PBS for 48 h. (B). A2780 cells were incubated with TRA2B siRNA 798, control or PBS for 48 h. The standard errors were calculated and plotted (left panels).

Supplementary Files

This is a list of supplementary files associated with this preprint. Click to download.

- Supplementaryfile.doc